Construction and Building Materials 351 (2022) 128831

Contents lists available at ScienceDirect

Construction and Building Materials

journal homepage: www.elsevier.com/locate/conbuildmat

Using Falling Weight Deflectometer (FWD) and Ground Penetrating Radar (GPR) to monitor the effects of seasonal moisture variation on the structural capacity of pavements

Thomas Calhoon [a,*], Eyoab Zegeye [a], Raul Velasquez [a], Jacob Calvert [b]

[a] Minnesota Department of Transportation, 1400 Gervais Ave, St Paul, MN 55109, USA
[b] Minnesota Department of Transportation, 9011 77th St NE, Otsego, MN 55362, USA

ARTICLE INFO

Keywords:
Falling-Weight Deflectometer (FWD)
Ground-Penetrating Radar (GPR)
Moisture variation
Unbound Aggregate Base (UAB)
Recycled Aggregate Base (RAB)
Non-Destructive Testing
Instrumentation
MnROAD

ABSTRACT

Moisture fluctuations in pavement foundation due to environmental conditions (e.g., heavy precipitation, freeze–thaw cycles, groundwater table variation, etc.) can significantly affect pavements' short- and long-term performance. Moisture variation in the pavement foundation is often monitored as a way to anticipate the structural capacity of pavements. Thus, the ability to monitor moisture variation through a proven non-destructive technology (NDT) such as Ground Penetrating Radar (GPR) would be beneficial for asset management by transportation agencies.

This paper summarizes the Minnesota Department of Transportation's (MnDOT) efforts at validating the use of GPR to monitor moisture in the pavement foundation through comparison with Falling-Weight Deflectometer (FWD) parameters that represent the structural condition of the pavement. The results in this paper are based on GPR, FWD and in-place moisture sensor data collected over 17 months on MnROAD instrumented test sections. The pavement test sections considered in this study included unbound aggregate bases (UAB) with virgin and recycled materials (i.e., RCA and RAP) covering a broad range of geotechnical behavior.

Previous efforts established a strong correlation between GPR-based moisture measurements and sensor-based moisture measurements. This correlation is further validated by investigating the relationship between GPR-based moisture measurements and FWD-based indices for structural capacity. The observed correlation is reasonable and in good agreement with the expected correlation between volumetric moisture content (VMC) of the base layer and the structural capacity of a pavement. This agreement validates the use of GPR to monitor moisture in pavement foundation. GPR is not a replacement for FWD, but it can be used in asset management efforts in addition to FWD to assess moisture fluctuation in pavement foundation during and after extreme environmental events (e.g., flooding, freeze-thawing) to determine when and where FWD testing may be necessary.

1. Introduction

It is known that high moisture content in the unbound aggregate base (UAB) layer of asphalt pavements can lead to reduced structural capacity and the creation of severe forms of pavement distress such as stripping, raveling, fatigue cracking, and/or permanent deformation [1]. In wet-freeze climates, the spring thawing period is typically accompanied by large variations in pavement moisture content. The influx of moisture requires transportation agencies to impose seasonal axle load restrictions on certain roads to avoid excessive road damage [2]. Generally, estimation of freezing and thawing indices from air temperature measurements and Falling Weight Deflectometer (FWD) deflection testing and analyses are performed on selected roads to establish proper time windows for the load restrictions. In Minnesota, spring load restriction (SLR) weeks generally fall between the end of February and the beginning of March. While FWD testing is necessary to monitor the effects of seasonal moisture fluctuations on the structural capacity of network-level roads, it is also expensive, time-consuming, disruptive to traffic, and limited in spatial coverage. It would be beneficial to have a tool that could frequently and efficiently monitor the

* Corresponding author at: 2510 Buchanan St NE, Minneapolis, MN 55418, USA
E-mail addresses: thomas.calhoon@state.mn.us (T. Calhoon), eyoab.zegeye.teshale@state.mn.us (E. Zegeye), raul.velasquez@state.mn.us (R. Velasquez), jacob.calvert@state.mn.us (J. Calvert).

https://doi.org/10.1016/j.conbuildmat.2022.128831
Received 15 March 2022; Received in revised form 14 July 2022; Accepted 14 August 2022

fluctuations to determine when FWD testing may be necessary.

In a recently published study [3] the feasibility of Ground Penetrating Radar (GPR) to monitor the seasonal moisture variation in base aggregate layers of in-service asphalt pavements was explored. The study was based on GPR and in-place sensor measurements collected over a 17-month period in four pavement test cells at the Minnesota Road Research Project (MnROAD) test facility. The study showed reasonable correlations between the dielectric constant (ε_r) of the base layers calculated from GPR data and the dielectric constant of the base layers measured by sensors installed in the pavement foundation. Furthermore, the Volumetric Moisture Content (VMC) of the aggregate base layers were calculated through empirical (Topp's equation) and material-specific calibration functions using the GPR-based and sensor-based dielectric constant values, respectively. The VMC values computed from the GPR and in-place sensors matched closely. These findings demonstrated the possibility of using GPR for spatially continuous (i.e., full-length coverage) and periodic monitoring of moisture variation in base layers of in-service roads. The present study aims to validate the use of GPR-based moisture measurements by exploring their relationship with FWD-produced structural capacity parameters. A relatively strong agreement between these two would be expected given the known relationship between pavement structural capacity and base layer moisture content.

2. Material and methods

The objective of this study was to investigate the correlation between GPR-based moisture measurements and FWD-based measurements of the structural capacity of asphalt pavements. This correlation was to be explored by analyzing GPR, FWD, and instrumentation measurements taken on three MnROAD test cells. This study used a single-channel GSSI 350 MHz ground-coupled (GC) GPR antenna operated in push mode and a Dynatest 8012 FastFWD model FWD unit.

Aggregate bases with virgin and recycled materials (i.e., RCA and RAP) covering a broad range of geotechnical behavior were investigated in this study. The three test sections used for this study (Cells 127, 188, and 189) have unique base materials and design structures. All three cells were built over a clay loam subgrade and surfaced with 90 mm of a similar asphalt concrete layer. For base material, cell 127 uses 152 mm of a dense-graded Minnesota aggregate material referred to as Class 6 (CL6). Cell 188 uses 305 mm of limestone material. Cell 189 uses 305 mm of an aggregate blend composed of Recycled Concrete Aggregate (RCA, approximately 80 %) and Recycled Asphalt Pavement (RAP, approximately 20 %). For subbase material, cell 127 uses 457 mm of Large Stone Subbase (LSSB). Cells 188 and 189 both use 90 mm of Select Granular Borrow (SGB). Cell 127 is approximately 79 m in length while cells 188 and 189 are approximately 61 m in length. Fig. 1 illustrates the cross-sectional profile views of the sections. This figure shows the locations of in-place capacitance sensors in the base, subbase, and subgrade layers. The moisture data considered in this study was generated by the sensors on the upper part of base layers (highlighted in green diamond markers). The depths of these highlighted sensors are: 165 mm for cell 127, 127 mm for cell 188, and 127 mm for cell 189. Index properties and gradations of the base, subbase, and subgrade materials investigated in this study are presented in Table 1 and Fig. 2, respectively.

FWD is a non-destructive evaluation (NDE) testing technology that is capable of measuring the deflection basin of a pavement surface subjected to specific point loads. FWD is commonly used due to its testing accuracy, repetitiveness, and realistic simulation of loading magnitude and duration [4]. The testing method consists of dropping a load of known weight from a target height and transmitting that load to the pavement through a circular loading plate [5]. The load plate is equipped with a load cell to measure the magnitude of the actual load transmitted to the pavement. The deformation of the road surface is measured using geophones located at set intervals from the loading point. The shape of the deformed pavement surface produced as a result of the loading constitutes the deflection basin of the pavement and can be used to evaluate the structural integrity and capacity of the pavement.

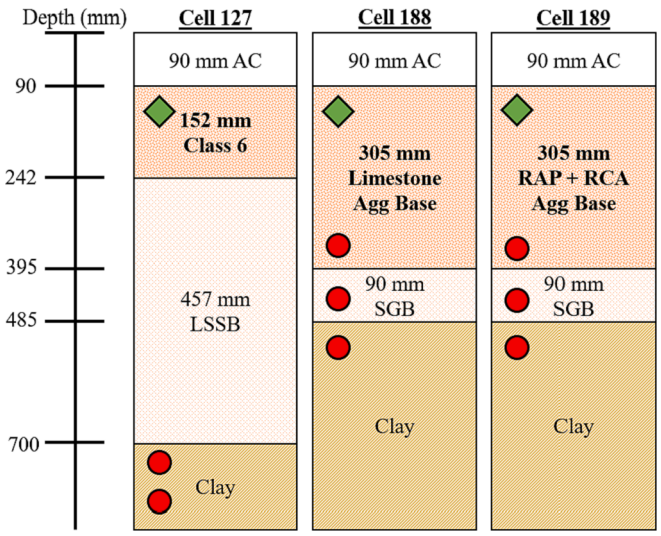

Fig. 1. Profile View of the Monitored MnROAD Test Cells. Sensors Used in This Study are Green Diamonds. (For interpretation of the references to colour in this figure legend, the reader is referred to the web version of this article.)

The GPR and FWD tests were performed over a 17-month period at intervals designed to capture Minnesota's different climatic seasons and particularly the winter-to-spring thawing season. Both GPR and FWD testing were conducted simultaneously on each day of testing (except for the first and last day of testing). A list of testing dates and the data available for each can be found in Table 2. Note that VMC_{5TE} is the sensor-based moisture measurement and VMC_{GPR} is the GPR-based moisture measurement. This testing schedule was predetermined based on the finding of a previous study [6], and focused on the critical freezing-thawing season.

2.1. Moisture fluctuation in the base layers

In-place capacitance-based sensors (i.e., Decagon 5TE) and GPR measurements were used to determine the average dielectric constant of the base layers at each testing date. A comprehensive discussion of the testing and analyses of the GPR data is discussed elsewhere [3]. In brief, for pavement applications, GPR is employed to transmit short electromagnetic (EM) wave pulses into the pavement system and record the back-reflected energy. The EM signal propagates through the different pavement layers at a speed determined by the layer's electromagnetic properties (i.e., dielectric permittivity, electrical conductivity, and magnetic permeability), which in turn are affected by the layer's physical and compositional properties (i.e., moisture content, density). Strong reflections (large amplitudes) are generated when the signal transitions from one layer to another with significantly different EM properties. Fig. 3 illustrates a GPR radargram image generated from the survey of cell 127. The y-axis in the radargram represents the GPR signals' time of travel in nanoseconds. The figure also shows that the GPR survey captures the upper and lower interfaces of the unbound aggregate layers. During the study [3], it was observed that the time distance between the interfaces varied depending on the moisture conditions of the pavement. This observation was used, along with the knowledge of the actual layer thicknesses and the time of travel or speed of propagation between consecutive layer interfaces, to determine the layer's dielectric constant at various moisture conditions. Given that the test sections and the GPR testing paths and configurations were held constant throughout the investigation period, the variations in the speed of

Table 1
Index Properties of Base, Subbase, and Subgrade Materials.

Material	Layer	Gravel (%)	Sand (%)	Fines (%)	C_u[i]	C_c[ii]	LL[iii]	PI[iv]	USCS[v]	AASHTO[vi]
Clay Loam	Subgrade	3.1	37.2	59.7	NA	NA	36.3	12.4	CL	A-6
SGB	Subbase	31.1	56.5	12.4	30.3	1.1	18.9	NP	SM	A-1-b
LSSB	Subbase	99.6	0.3	0.1	1.84	1.08	NA	NP	GP	A-1-a
Limestone	Base	52.3	32.6	15.1	211.3	1.91	17.9	NP	GM	A-1-b
RCA + RAP	Base	41	50.4	8.6	49.41	0.98	27.4	NP	SP-SM	A-1-a
Class 6	Base	35.1	58.6	6.3	23.82	0.6	27.4	NP	SP-SM	A-1-a

[i] Uniformity Coefficient
[ii] Coefficient of Curvature
[iii] Liquid Limit
[iv] Plasticity Index
[v] Unified Soil Classification System Classification
[vi] American Association of State Highway and Transportation Officials Classification

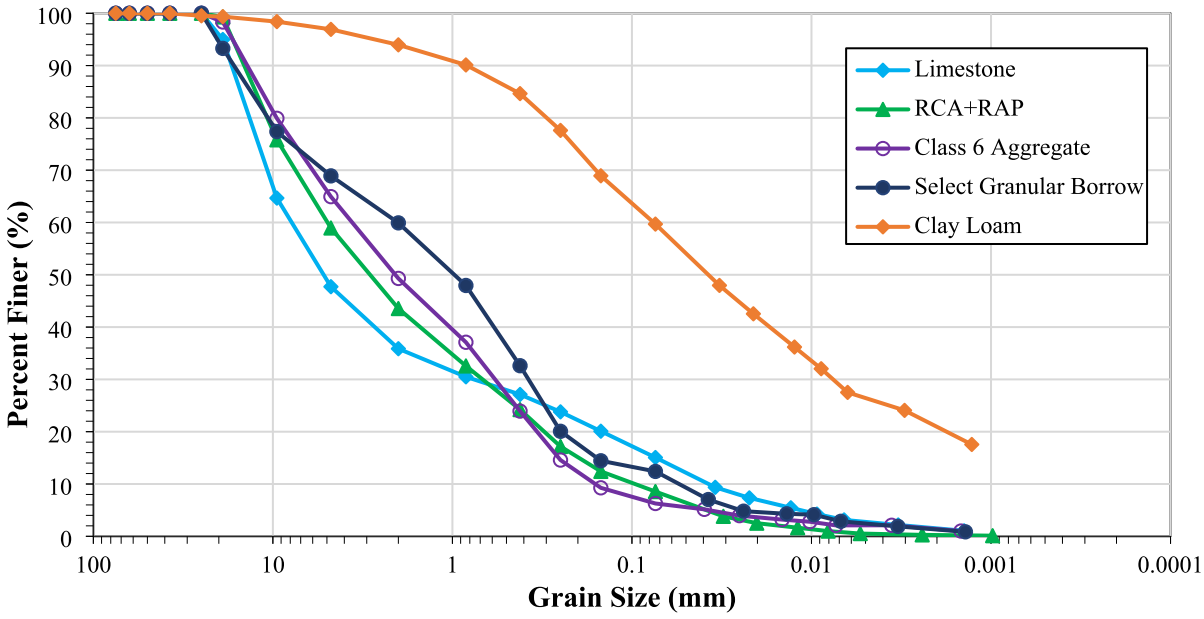

Fig. 2. Gradation of Base, Subbase, and Subgrade Materials.

Table 2
Testing Dates and Data Availability.

Date	Data Availability		
	VMC_{5TE}	VMC_{GPR}	FWD
2/24/2020			x
3/6/2020	x	x	x
3/13/2020	x	x	x
3/17/2020	x	x	x
3/26/2020	x	x	x
5/8/2020	x	x	x
10/29/2020	x	x	x
11/20/2020	x	x	x
12/8/2020	x	x	x
1/21/2021	x	x	x
2/19/2021	x	x	x
3/4/2021	x	x	x
3/11/2021	x	x	x
3/25/2021	x	x	x
4/15/2021	x	x	x
5/13/2021	x	x	x
6/16/2021			x

propagation of the GPR signals were attributed to the fluctuation in moisture content. Hence, a GPR signal analysis algorithm was developed to determine the average dielectric constant of the base layers at each testing date. It should be noted that while GPR data was collected along the entire length of each of the tested cells, only the data 15 m on each side of the midpoint of the cell was used to measure the moisture in the base layer.

The dielectric constant values were then converted to volumetric moisture content (VMC) through, the Topp's equation (Equation (1)) and a material-specific calibration function (Equation (2)), respectively, for GPR and in-place sensor dielectrics. The coefficients for Equation (2) are presented in Table 3.

$$VMC_{GPR} = -0.053 + 0.0292*\varepsilon_r - 5.5*10^{-4}*\varepsilon_r^2 + 4.3*10^{-6}*\varepsilon_r^3 \quad (1)$$

$$VMC_{5TE} = b + a*\varepsilon_r \quad (2)$$

The seasonal moisture fluctuation within the base layer of cells 127, 188, and 189 (as measured by the installed sensors) can be seen in Figs. 4-6. The plots in these figures also contain precipitation, the optimum moisture content (OMC) measured in the laboratory, and the upper (UB) and lower (LB) bounds of the in-situ moisture content measured using Nuclear Density Gauge (NDG) right after the construction of the pavement foundation. The GPR-based moisture measurements from each day of testing are also displayed on these plots. Figs. 4-6 indicate that moisture in aggregate base measured with instrumentation and during construction (dashed dark lines) generally agree and are typically below the optimum moisture content (OMC). This is encouraging for the validation of GPR-based moisture measurements. The

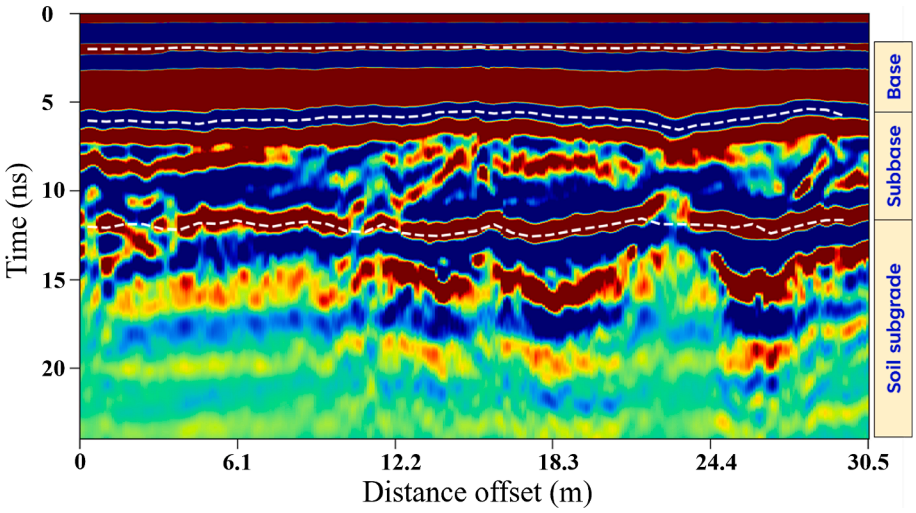

Fig. 3. MnROAD Cell 127 GPR radargram image.

Table 3
MnROAD Material-Specific Calibration Coefficients for Decagon 5TE Moisture Sensors.

Base Material	a	b	Cell
CL 6	0.0006	−0.1438	127
Limestone	0.0003	−0.0437	188
RAP + RCA	0.0006	−0.1358	189

upper and lower bounds of moisture during construction and the OMC given in these plots are static measurements that were taken during the initial construction period and do not reflect seasonal moisture variation. They are meant as a check on the collected data to ensure it is reasonable. Further, the figures indicate that instrumentation was able to capture the influx of water from heavy precipitation events as indicated by the spikes in sensor response after a rain event. Time histories from moisture sensors show that in general, the pavement structures recover to steady-state condition fairly quickly after a heavy rain event.

The most dramatic period of change in the moisture results is during spring thawing. The moisture drops to residual moisture content during winter conditions (January and February for 2021), then rapidly increases with the spring thaw. The spikes in moisture at the beginning of spring represent the spring-thaw period [3].

As indicated in a previous study [3], Fig. 7 indicates a relatively good agreement between the GPR-based and sensor-based moisture measurements.

2.2. FWD testing

The FWD tests were performed at ten midlane locations in the trafficked lane of each cell. The location of the FWD test points, GPR collection, and moisture sensors within the three tested cells can be

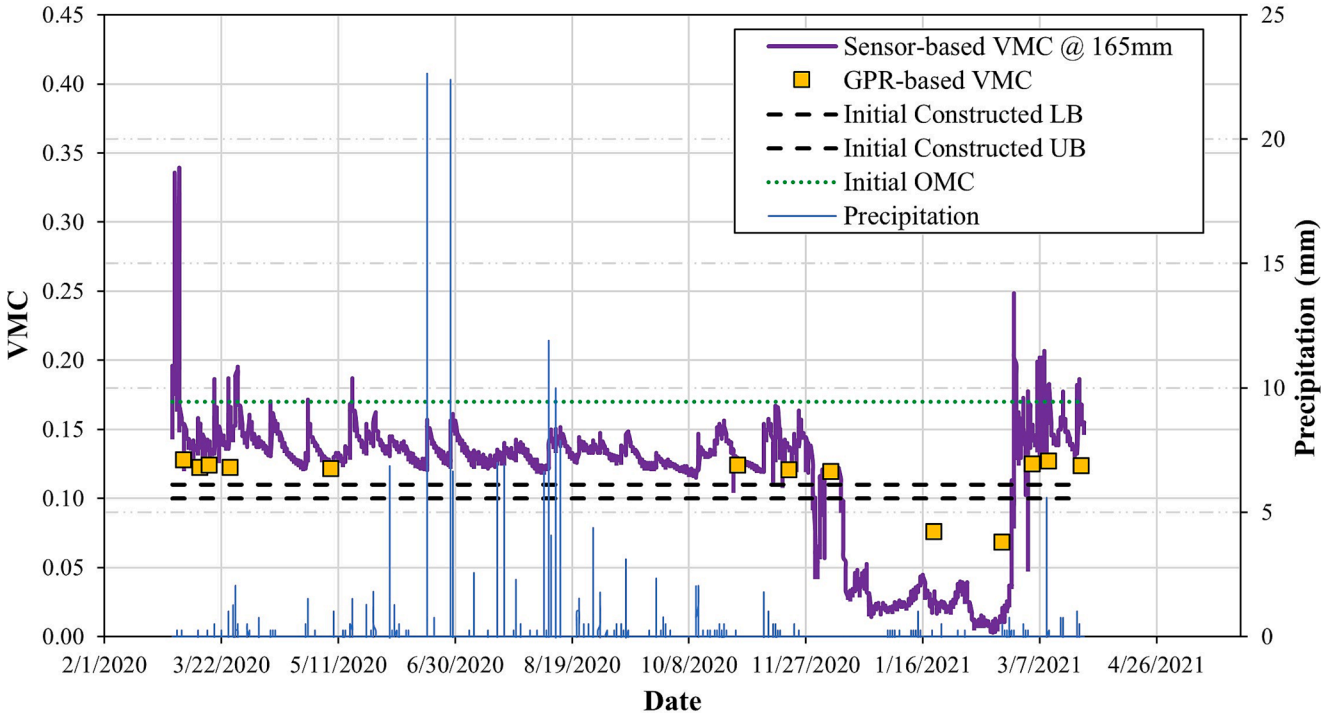

Fig. 4. MnROAD Cell 127 Moisture Monitoring.

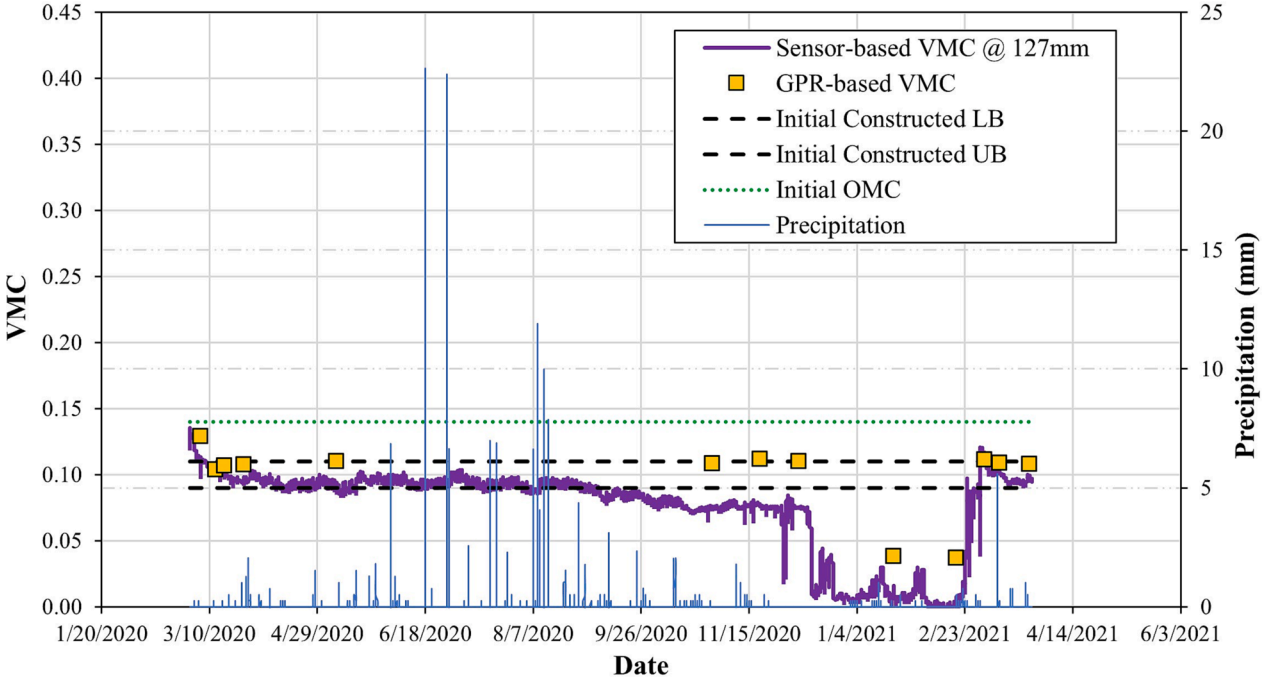

Fig. 5. MnROAD Cell 188 Moisture Monitoring.

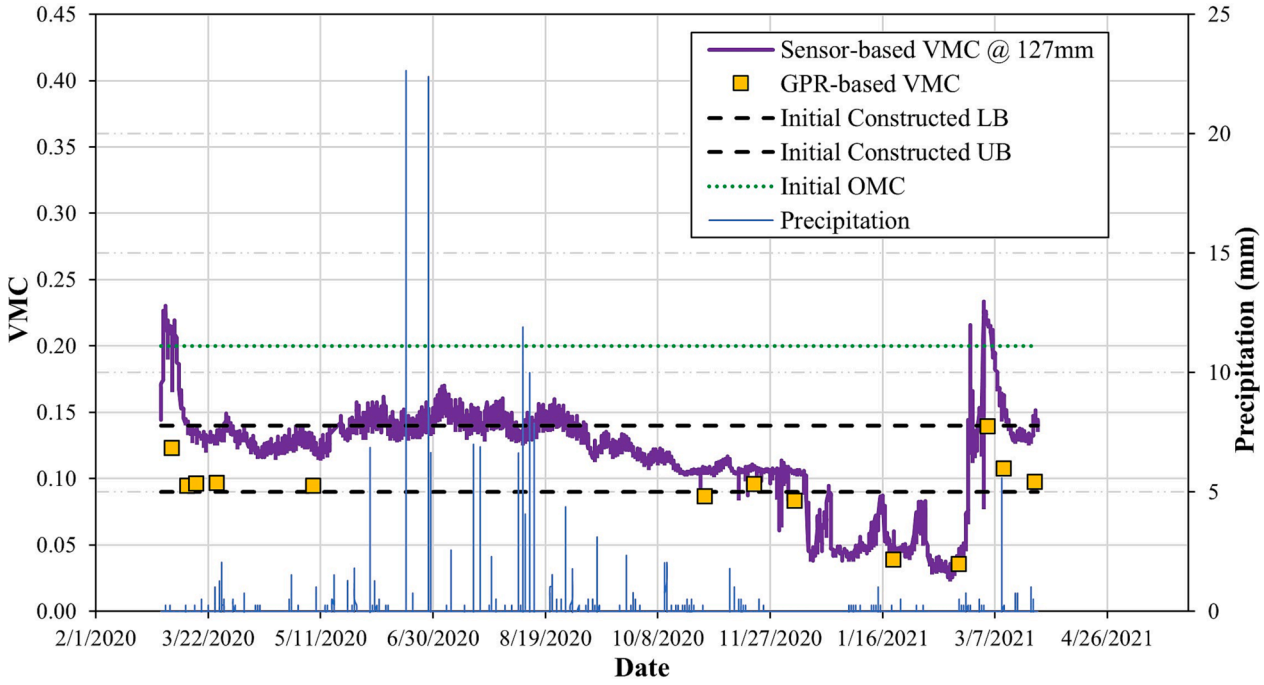

Fig. 6. MnROAD Cell 189 Moisture Monitoring.

found in Fig. 8. Three drops were performed for each test, but only the data from the second drop, which had a target load of 40 kN, was used for this study. The FWD unit uses a 152 mm grooved loading plate and the standard nine-sensor geophone spacing for Long-Term Pavement Performance Program (LTPP) testing [7]. Each test used the first three drops of the standard LTPP flexible testing drop sequence. The FWD unit contains sensors that enable it to measure the air temperature and the surface temperature of the pavement at the time of the test.

2.3. *Data processing*

There are two standard approaches to analyzing FWD data. The first one relies on employing layered elastic principles (i.e., ELMOD) combined with finite element simulations (i.e., TONN2010, MODULUS 7.0) to back-calculate the elastic moduli and stiffnesses of the pavement layers from the magnitude and shapes of the FWD deflection basins. Generally, these tools take as input the layer thicknesses and the FWD basin deflection and back-calculate the layer moduli. Although these approaches are known to produce reliable stiffness estimates, especially

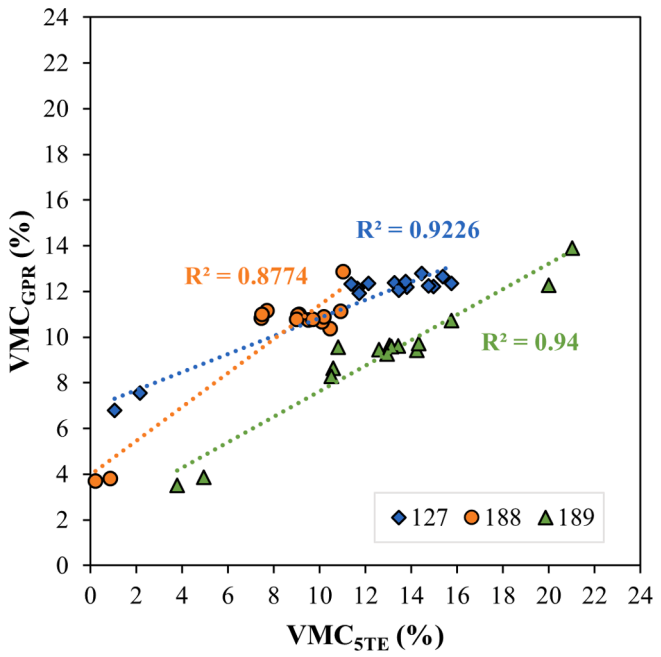

Fig. 7. Linear Correlation of GPR-Based and Sensor-Based Moisture Measurements.

for the top bituminous layer, they do not entirely account for the elastoplastic response (i.e., shear yielding) of UAB and the associated change in stiffness and shear strength from moisture fluctuations. Additionally, as it was observed in this study, during winter freezing conditions, the pavement layers are significantly stiffer, and the deflections are not sufficiently large enough to distinguish the individual layer moduli through back-calculation.

An alternative approach consists in utilizing FWD deflection parameters directly computed from the geometry of the deflection basin. These parameters include temperature-adjusted deflection directly beneath the applied load ($D0_{adj}$), Structural Capacity Index (SCI), Base Damage Index (BDI), Base Curvature Index (BCI), Deflection Ratio (DR), F-1 shape factor, and F-2 shape factor. Given the limitations of the back-calculation approaches discussed in the above paragraph, this second approach was found more suitable for the present study.

The data processing started with verifying the reasonableness of the individual basin deflections. For each test date and test cell, the basin deflections were statistically compared. The average and standard deviation D0 of the basin deflections were calculated. Basin deflections with D0 measurements that were further than ± one standard deviation from the average were flagged and eventually removed. Fig. 9 shows a comparison of the basin deflections before and after the filtering.

The accepted FWD basin deflections were used to calculate the FWD basin parameters. Finally, the average of the FWD parameters was considered to represent the test cell at the given test date. The calculation of each of those parameters and their significance is detailed below.

The temperature of the asphalt bituminous layer and the moisture (i.e., content and condition) of the unbound aggregate layer are known to be the most critical factors affecting the FWD deflection measurements. This study is concerned with the relationship between moisture and pavement structural capacity. Therefore, it is important to remove the effects of temperature from the deflection measurements to better isolate the effects of moisture. The effect of the temperature is mainly due to the viscoelastic nature of the bituminous layer and is more pronounced closer to the center of loading [8–10]. Park *et al.* [9] found that

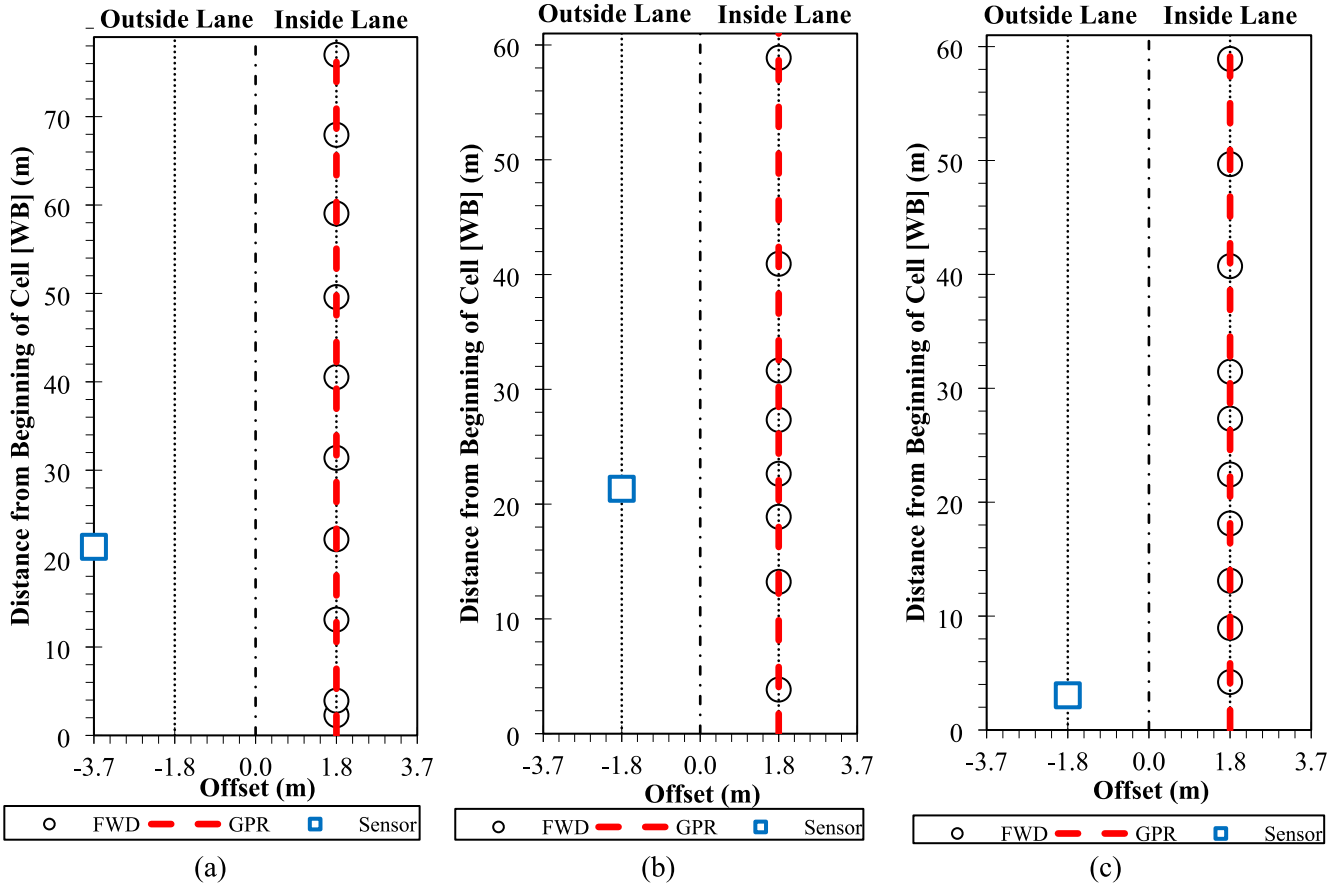

Fig. 8. Location of FWD test points, GPR collection, and moisture sensors within test cells (a) 127, (b) 188, and (c) 189.

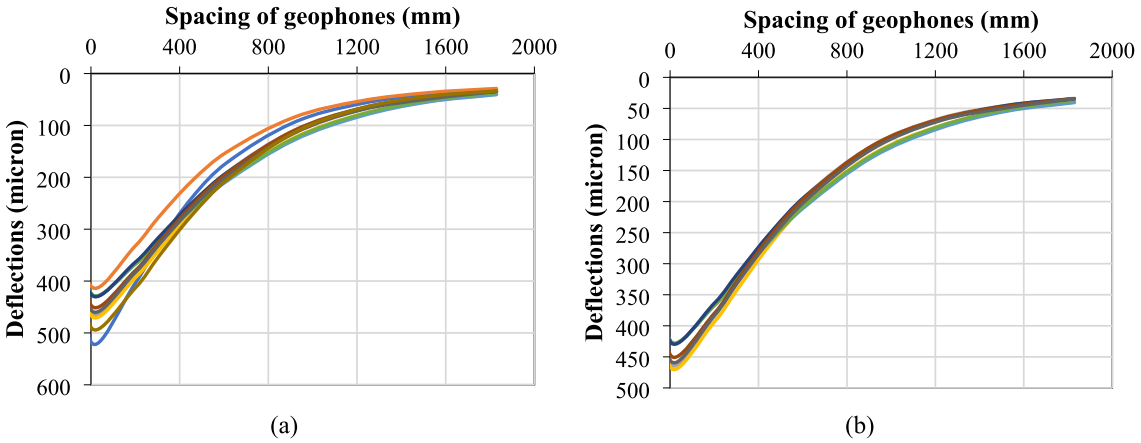

Fig. 9. FWD Basin deflections collected from one cell in one day (a) before and (b) after outlier removal.

the radial distance in which the temperature within the asphalt layer affects deflection is smaller for thin asphalt layers. Therefore, not all sensors readings needed temperature correction. Only the deflection measurement directly beneath the load requires adjustment for this study due to the relatively thin asphalt surface layers of the tested cells (90 mm) compared to the distance of the next geophone (305 mm).

The temperature-adjusted (reference in-pavement temperature of 22.2 °C) deflection directly beneath the load, $D0_{adj}$, is calculated with Equation (3) [11]. This equation requires knowledge of the temperature within the asphalt layer during the FWD test. In place of temperature data from installed sensors, the internal asphalt layer temperature (at a depth of 1/3 the asphalt thickness) was predicted with the BELLS3 temperature model shown in Equation (4). Although the FWD unit used LTPP guidelines for sensor spacing and drop sequence, the time duration of the testing more closely matched routine testing methods, making the use of BELLS3 most appropriate [12]. Use of this equation, and, specifically, of the two variations of the 18-hr sine function within it, are discussed further in the literature [12].

$$D0_{adj} = D0*10^{(C0+A*r)*(T_{bells}*H_{ac})} \tag{3}$$

where:

r = Radial distance from center of load plate (is equal to 0).
A = Regression Constant (is equal to $-5.47*10^{-8}$).
$C0$ = Regression Constant (is equal to $4.65*10^{-5}$).
T_{bells} = Pavement temperature at 1/3 predicted by BELL3 (°C).
H_{ac} = Thickness of asphalt pavement layer (mm).

$$T_{bells} = 0.95 + 0.892*T_{surf} + \left(\log_{10}\left(\frac{H_{ac}}{3}\right) - 1.25\right)*\left(-0.448*T_{surf} + 0.621*T_{prev} + 1.83*\sin(hr_{18} - 15.5)\right) + 0.042*T_{surf}*\sin(hr_{18} - 13.5) \tag{4}$$

where:

T_{surf} = Pavement surface temperature (°C).
T_{prev} = Average air temperature the day before testing (°C).
$\sin(hr_{18} - 15.5)$ = 18-hr sine function, 15.5 variation.
$\sin(hr_{18} - 13.5)$ = 18-hr sine function, 13.5 variation.

To the knowledge of the authors, there is no known moisture correction function for FWD parameters. The present study would provide insight into that since it aims to isolate and detect the effect of moisture by testing the same pavement structure at different subsurface moisture levels and conditions (e.g., frozen). Details for the remaining FWD parameters can be found in Table 4.

3. Results and discussion

To best capture the correlation between FWD parameters and the seasonal moisture variation, it is best to look at how the FWD parameter results change with time. Figs. 10-12 show the average monthly results for three of the FWD parameters. The results for each cell are separated to allow for a better understanding of how the unique material and structural properties of the cells affect their results. It is clear from these plots that cold winter conditions have a drastic effect on the stiffness of the asphalt pavement. Because the D0 measurements were corrected for temperature using Equation (3), the seasonal changes observed in Figs. 10-12 can be attributed to changes in the base moisture content (i.e., due to the freeze–thaw phenomenon). The temperature data provided in these figures is from a temperature sensor within the base layer at a depth of 102 mm and indicates when freezing and thawing may occur. The winter to spring period contains the most dramatic changes in the value of most of the FWD parameters. However, the parameters more associated with the upper asphalt pavement layer ($D0_{adj}$) seem to show continued growth into the summer. The parameters associated with the lower pavement layers (BDI, $F\text{-}2_{alt}$) peak in the thaw period and show a decline into the summer.

While the seasonal trends of the FWD parameters and GPR-based moisture match reasonably well, the BDI and $F\text{-}2_{alt}$ FWD parameters showed the most significant agreement. This finding is encouraging for the validation of GPR-based moisture measurements given the known relationship between the moisture in the base layer and the structural condition of the base layer. The linear correlation between these parameters and the moisture measured with instrumentation and GPR can be seen in Figs. 13 and 14. The correlations involving sensor-based and GPR-based moisture measurements are comparable. It should be noted that patterns that may appear within data clusters (e.g., winter measurements) are not captured by using an overall linear regression.

Fig. 13a and 14a show that cells 188 and 189 have similar trends. Cells 188 and 189 have similar pavement profiles in comparison to Cell 127 as shown in Fig. 1. Normalizing BDI and $F\text{-}2_{alt}$ by the base layer thickness of the respective cell results in a relatively strong agreement between the FWD parameters results from all cells and the GPR-based moisture. This can be seen in Fig. 15. The thickness-normalized FWD parameters show weaker agreement with the sensor-based moisture data as opposed to the GPR-based moisture data. This can be seen in Fig. 16. The benefit of thickness-normalization on the correlation of GPR-based moisture and the FWD parameters makes sense as the calculation of the GPR-based moisture is dependent on the thickness of the base layer.

The relatively strong linear correlation between moisture measurements calculated from GPR data and base layer structural capacity measurements from FWD validates the previously-established

Table 4
All FWD Parameters Except $D0_{adj}$.

Parameter	Name	Formula	Meaning	Sources	Equation #
SCI	Structural Capacity Index	$SCI = D0_{adj} - D_{305mm}$	Indication of the structural condition of the upper bituminous layer	[4,5,13,14]	5
BDI	Base Damage Index	$BDI = D_{305mm} - D_{610mm}$	Indication of the structural condition of the granular base and subbase layers	[5,13,14,16]	6
BCI	Base Curvature Index	$BCI = D_{610mm} - D_{914mm}$	Indication of the structural condition of the subgrade	[13,14]	7
DR	Deflection Ratio	$DR = \frac{D_{610mm}}{D0_{adj}}$	Measure of how flat the upper portion of the deflection basin is	[4,15]	8
F-1	Shape Factor	$F-1 = \frac{D0_{adj} - D_{610mm}}{D_{305mm}}$	Normalized representation of the amount of curvature in the upper portion of the deflection basin	[12,13,16,17]	9
F-2	Shape Factor	$F-2 = \frac{D_{305mm} - D_{914mm}}{D_{610mm}}$	Normalized representation of the amount of curvature in the lower portion of the deflection basin	[13,16]	10
$F\text{-}2_{alt}$	Shape Factor	$F-2_{alt} = \frac{D_{610mm} - D_{914mm}}{D_{610mm}}$	Normalized measure of change in deflection between 2ft and 3ft away from the load		11

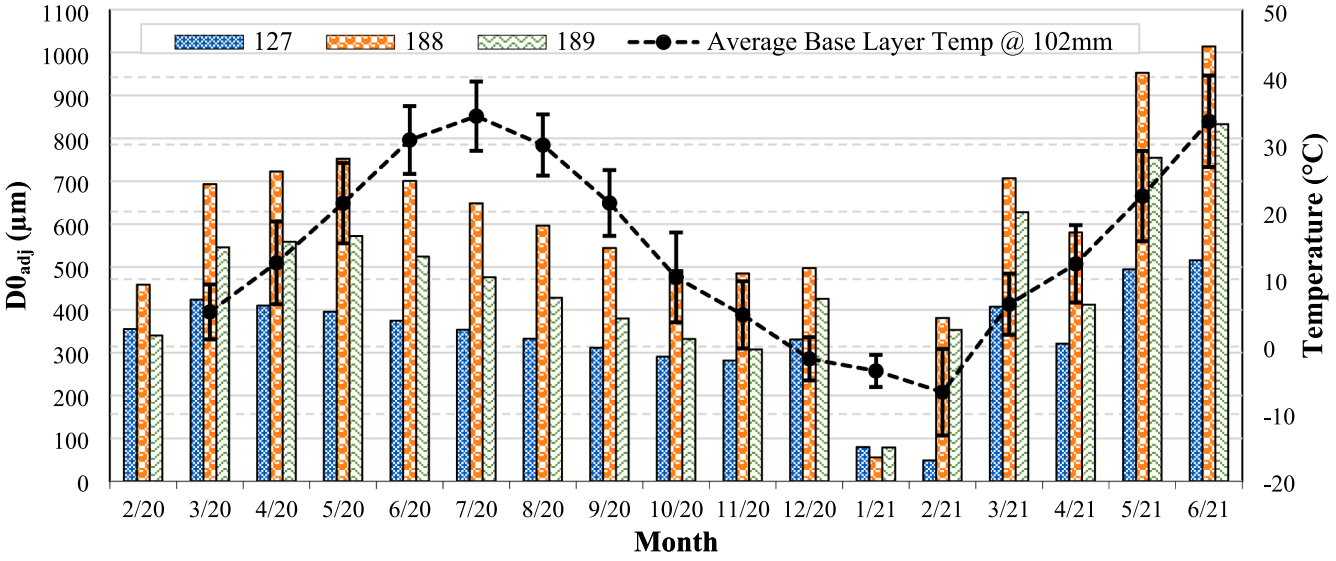

Fig. 10. Month-by-Month Results for $D0_{adj}$.

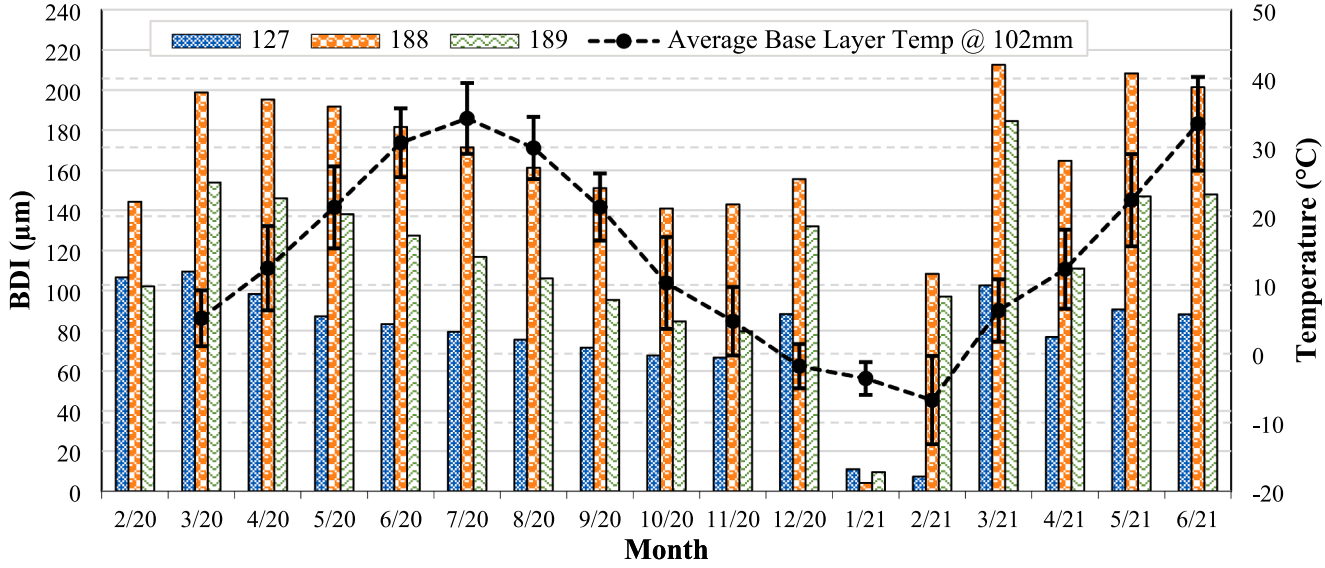

Fig. 11. Month-by-Month Results for BDI.

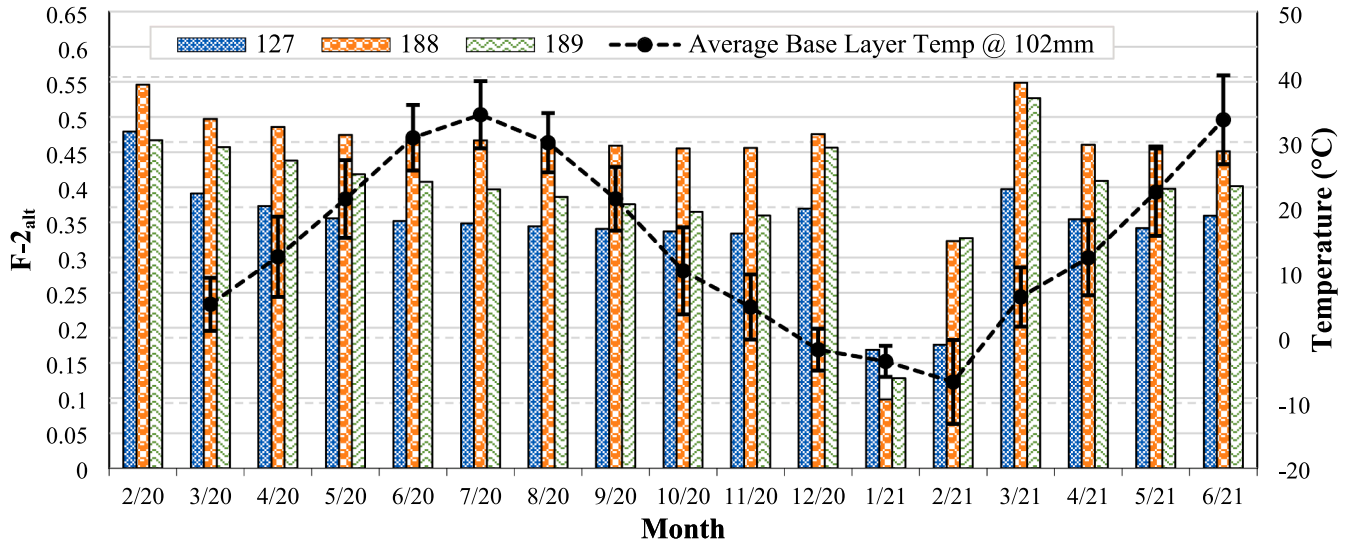

Fig. 12. Month-by-Month Results for F-$2_{alt.}$

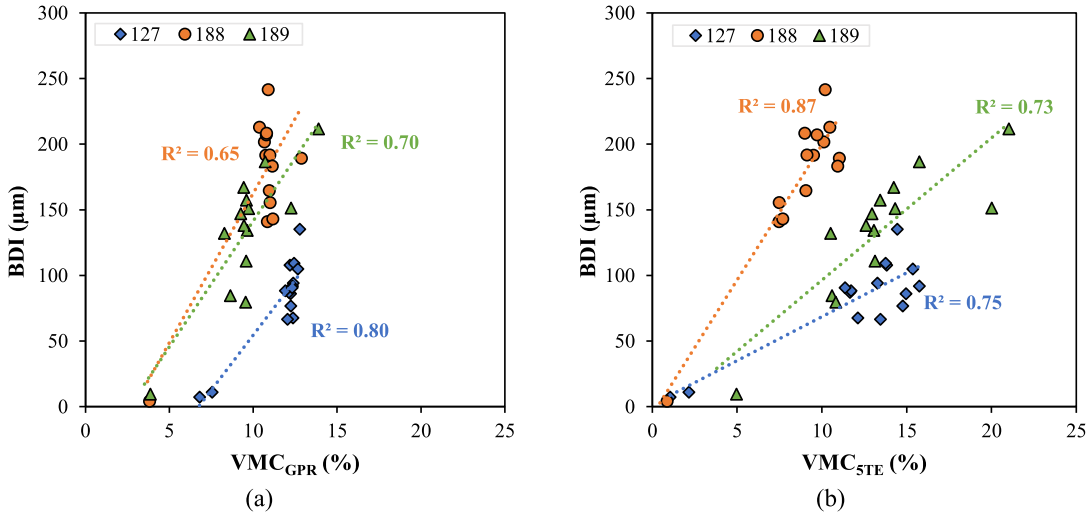

Fig. 13. Linear Correlation of BDI with (a) GPR-Based Moisture and (b) Sensor-Based Moisture.

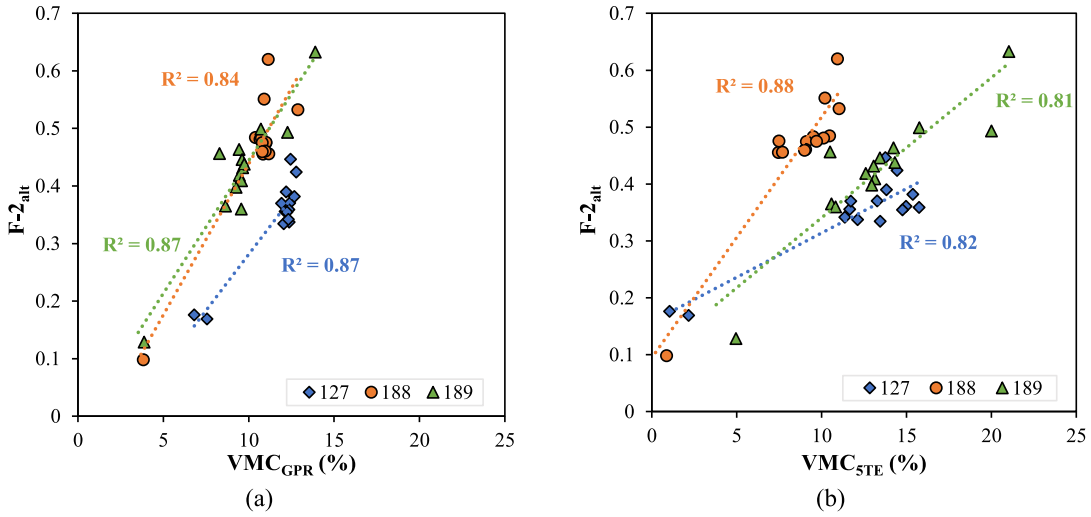

Fig. 14. Linear Correlation of F-2_{alt} with (a) GPR-Based Moisture and (b) Sensor-Based Moisture.

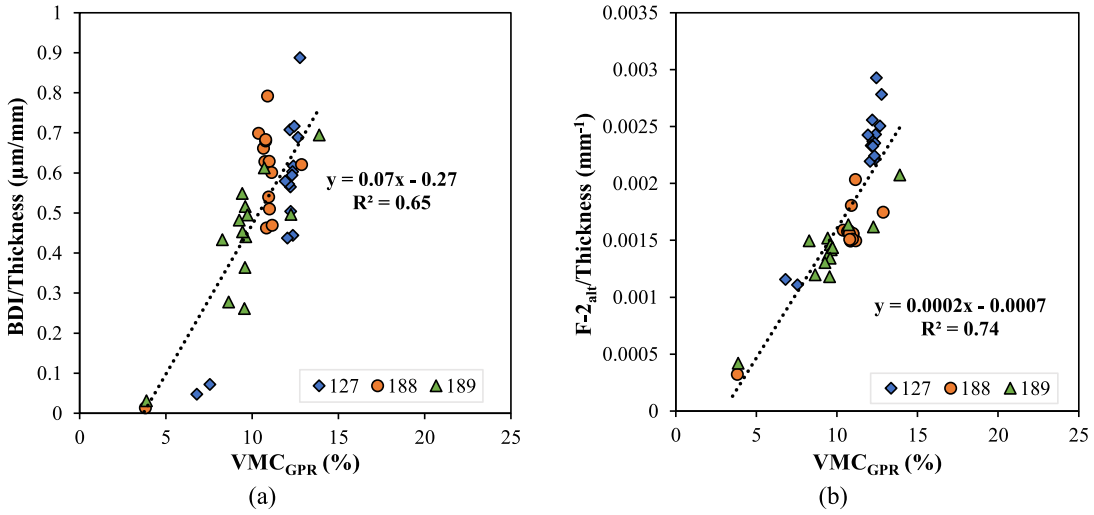

Fig. 15. Linear Correlation of GPR-Based Moisture Data with (a) Thickness-Normalized BDI and (b) Thickness-Normalized F-$2_{alt.}$

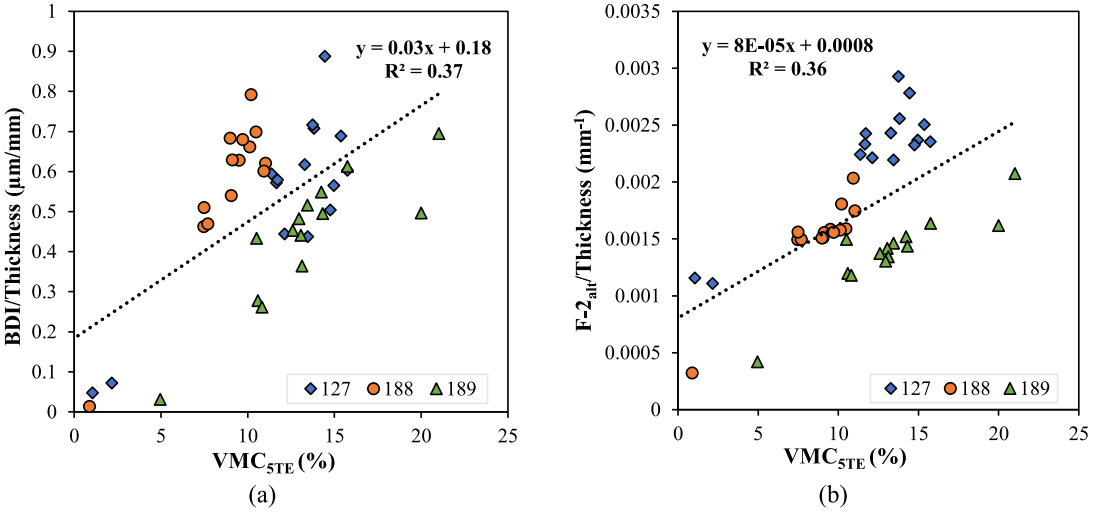

Fig. 16. Linear Correlation of Sensor-Based Moisture Data with (a) Thickness-Normalized BDI and (b) Thickness-Normalized F-$2_{alt.}$

correlation between GPR-based and sensor-based moisture measurements. It also shows the potential for the use of GPR to continuously and efficiently monitor seasonal moisture variations in support of efforts to determine the structural condition of asphalt pavements with FWD. During periods of expected moisture fluctuation, regular GPR testing may be used to monitor for changes in the pavement foundation VMC and to identify critical sections. This would allow for more strategic use of FWD testing.

4. Conclusions

This study explores the correlation between FWD-produced structural capacity parameters and GPR-based moisture measurements obtained from an extensive monitoring program of three MnROAD test cells over a roughly-two-year period covering extreme seasonal variations. A relatively strong correlation between these two would be expected given the known relationship between pavement structural capacity and base layer moisture content and would validate the use of GPR to monitor moisture in the pavement foundation. Unbound aggregate bases investigated were built with virgin and recycled materials to cover a broad range of geotechnical behavior.

The two FWD parameters that showed the most significant correlation with the GPR-based moisture measurements were the Base Deflection Index (BDI) and the alternate F-2 shape factor. These two parameters indicate the structural condition of the base layer. Normalizing the FWD parameters results by the base layer thickness of their respective test cell results in a relatively strong correlation with the GPR-based moisture when considering the data from all cells at once. These findings show a relatively strong correlation between the GPR-based moisture measurements and FWD-based indices of structural capacity. It also shows the potential for the use of GPR to rapidly monitor seasonal moisture fluctuation to determine where and when FWD structural capacity testing should take place.

Author statement

The authors confirm contribution to the paper as follows: study conception and design: Eyoab Zegeye; data collection: Micah Holzbauer, Jacob Calvert, and Raul Velasquez; data processing and interpretation of results Eyoab Zegeye, Thomas Calhoon and Raul Velasquez; draft manuscript preparation: Thomas Calhoon, Eyoab Zegeye, Raul Velasquez, and Jacob Calvert. All authors reviewed the results, contributed to the article, and approved the final version of the manuscript.

CRediT authorship contribution statement

Thomas Calhoon: Writing – original draft, Writing – review & editing, Formal analysis, Visualization. **Eyoab Zegeye:** Conceptualization, Methodology, Writing – original draft, Writing – review & editing, Formal analysis, Visualization. **Raul Velasquez:** Investigation, Writing – original draft, Writing – review & editing, Formal analysis, Visualization. **Jacob Calvert:** Investigation, Writing – original draft.

Declaration of Competing Interest

The authors declare that they have no known competing financial interests or personal relationships that could have appeared to influence the work reported in this paper.

Data availability

Data will be made available on request.

Acknowledgments

This article is based upon work fully supported by the Minnesota Department of Transportation (MnDOT)'s Office of Materials and Road Research (OMRR): MNDOT Operational fund 2700 FIN T7936500. The authors gratefully acknowledge the support. However, the findings, opinions, and recommendations expressed in this publication are those of the authors and do not necessarily reflect the views of MnDOT. The authors gratefully acknowledge Micah Holzbauer for assisting in gathering the GPR data used in this study, Leonard Palek for the installation and calibration of geotechnical instrumentation, and Shongtao Dai for his leadership and technical insights. The authors would also like to acknowledge the support provided by the Office of Materials and Road Research (OMRR) leadership and MnROAD Operations staff.

References

[1] Y.R. Kim, J.S. Lutif, A. Bhasin, D.N. Little, Evaluation of moisture damage mechanisms and effects of hydrated lime in asphalt mixtures through measurements of mixture component properties and performance testing, J. Mater. Civ. Eng. 20 (10) (2000) 659–667, https://doi.org/10.1061/(asce)0899-1561(2008)20:10(659).

[2] Bly, P., Thompkins, D., & Khazanovich, L. (2010). *Allowable Axle Loads on Pavements* (Report No. MN/RC 2011-02). Minnesota Department of Transportation. https://conservancy.umn.edu/bitstream/handle/11299/150095/Mn_DOT2011-02.pdf?sequence=1&isAllowed=y.

[3] E. Zegeye-Teshale, M. Holzbauer, S. Dai, Using ground penetrating radar to monitor seasonal moisture fluctuations in base layers of existing roads transportation research record, J. Trans. Research Board. 2676 (6) (2022) 371–386.

[4] O. Talvik, A. Aavik, Use of FWD Deflection Basin Parameters (SCI, BDI, BCI) for pavement condition assessment, The Baltic J. Road and Bridge Eng. 4 (4) (2009) 196–202, https://doi.org/10.3846/1822-427X.2009.4.196-202.

[5] U.J. Solanki, P.J. Gundaliya, M.D. Barasara, Structural Evaluation of Flexible Pavement Using Falling Weight Deflectometer, in: P.N. Tekwani, M. Bhavsar, B. A. Modi (Eds.), Multi-disciplinary Sustainable Engineering: Current and Future Trends, CRC Press, 2016, pp. 141–146.

[6] E. Zegeye Teshale, D. Shongtao, L.F. Walubita, Evaluation of unbound aggregate base layers using moisture monitoring data, Trans. Research Record: J. Trans. Research Board 2673 (3) (2019) 399–409.

[7] Schmalzer, P. N. (2006). *Long-Term Pavement Performance Program Manual for Falling Weight Deflectometer Measurements, Version 4.1* (Report No. FHWA-HRT-06-132). Federal Highway Administration. https://www.fhwa.dot.gov/publications/research/infrastructure/pavements/ltpp/06132/06132.pdf.

[8] D.H. Chen, J. Bilyeu, H.H. Lin, M. Murphy, Temperature correction on falling weight deflectometer measurements, Trans. Research Record: J. Trans. Research Board 1716 (1) (2000) 30–39, https://doi.org/10.3141/1716-04.

[9] H.M. Park, Y.R. Kim, S. Park, Temperature correction of multiload-level falling weight deflectometer deflections, Trans. Research Record: J. Trans. Research Board 1806 (2002) 3–8, https://doi.org/10.3141/1806-01.

[10] Straube, E., & Jansen, D. Temperature Correction of Falling Weight Deflectometer Measurements. In Tutumluer, E. & Al-Qadi I. L. (Eds.), *Bearing capacity of roads, railways and airfields: proceedings of the 8th international conference on the bearing capacity of roads, railways and airfields, Champaign, Illinois, USA, June 29-July 2, 2009* (pp. 789-798). CRC Press.

[11] Kim, Y. R., & Park. H. M. (2002). *Use of FWD Multi-Load Data for Pavement Strength Estimation* (Report No. FHWA/NC/2002-006). Federal Highway Administration. https://rosap.ntl.bts.gov/view/dot/5253.

[12] Lukanen, E. O., Stubstad, R., & Briggs, R. (2000). *Temperature Predictions and Adjustment Factors for Asphalt Pavements* (Report No. FHWA-RD-98-085). Federal Highway Administration. https://www.fhwa.dot.gov/publications/research/infrastructure/pavements/ltpp/98085a/98085a.pdf.

[13] Horak, E. (1987). *Aspects of Deflection Basin Parameters Used in A Mechanistic Rehabilitation Design Procedure for Flexible Pavements in South Africa.* [Doctoral dissertation, University of Pretoria]. Institutional Repository of the University of Pretoria.

[14] E. Horak, Benchmarking the structural condition of flexible pavements with deflection bowl parameters, J. South African Institution of Civil Eng. 50 (2) (2008) 2–9. http://www.scielo.org.za/pdf/jsaice/v50n2/01.pdf.

[15] G.W. Chai, G. Lewer, G. Cancian, A Study of the FWD Deflection Characteristics of Composite and Sandwich Pavements, in: K.A.H. Kyōkai (Ed.), The 11th International Conference on Asphalt Pavements, August 1 to 6, 2010, Nagoya, Aichi, Japan: Proceedings, International Society for Asphalt Pavements, 2010.

[16] Kim, Y. R., Lee, Y. C., & Ranjithan, S. R. (2000). Flexible Pavement Condition Evaluation Using Deflection Basin Parameters and Dynamic Finite Element Analysis Implemented by Artificial Neural Networks. In Tayabji, S. D., Lukanen, E. O. (Eds.), *Nondestructive Testing of Pavements and Backcalculation of Moduli: Third Volume* (pp. 514-530). ASTM.

[17] Pierce, L. M., Bruinsma, J. E., Smith, K. D., Wade, M. J., Chatti, K., & Vandenbossche, J. M. (2017). *Using Falling Weight Deflectometer Data with Mechanistic-Empirical Design and Analysis, Volume III: Guidelines for Deflection Testing, Analysis, and Interpretation* (Report No. FHWA-HRT-16-011). Federal Highway Administration. https://www.fhwa.dot.gov/publications/research/infrastructure/pavements/16011/16011.pdf.